ELSEVIER

Biochimica et Biophysica Acta 1563 (2002) 29–34

BIOCHIMICA ET BIOPHYSICA ACTA
BBA

www.bba-direct.com

The effect of hydrostatic pressure on S-layer-supported lipid membranes

Bernhard Schuster *, Uwe B. Sleytr

Center for Ultrastructure Research and Ludwig-Boltzmann-Institute for Molecular Nanotechnology, Universität für Bodenkultur Wien, Gregor-Mendel-Straße 33, 1180 Vienna, Austria

Received 9 October 2001; received in revised form 5 February 2002; accepted 21 February 2002

Abstract

We report on the behavior of unsupported and surface layer (S-layer)-supported lipid membranes at the application of a uniform hydrostatic pressure. At a hydrostatic pressure gradient higher than 6 N/m^2, unsupported lipid membranes, independent from which side pressurized and S-layer-supported lipid membranes pressurized from the lipid-faced side revealed a pronounced increase in capacitance. A maximal hydrostatic pressure gradient of 11.0 N/m^2 resulted in an almost doubling of the capacitance of the (composite) membranes. S-layer-supported lipid membranes showed a hysteresis in the capacitance versus pressure plot, indicating that this composite structure required a certain time to reorient when the pressure gradient acting from the lipid-faced side was balanced. By contrast, the S-layer-supported lipid membrane pressurized from the protein-faced side revealed only a minute increase in capacitance ($C/C_{0,\max} = 1.17 \pm 0.05$), reflecting only minor pressure-induced area expansion. In addition, no hysteresis could be observed, indicating that no rearrangement of the composite membrane occurred. The maximal induced tension was with 4.3 ± 0.2 mN/m, significantly higher than that of unsupported (2.5 ± 0.3 mN/m) and S-layer-supported lipid membranes pressurized from the lipid-faced side (2.6 ± 0.1 mN/m).

Keywords: Crystalline bacterial surface layer (S-layer); Planar supported lipid membrane; Hydrostatic pressure

1. Introduction

Crystalline proteinaceous cell surface layers (S-layers) represent the outermost cell envelope component in organisms of almost every taxonomic group of walled bacteria and archaea [1–3]. The S-layer from *Bacillus coagulans* E38-66/v1, used in the present study, represents a highly specialized supramolecular structure and is composed of identical, nonglycosylated protein subunits with a molecular weight of 100.000. The S-layer lattice is a highly porous structure (Fig. 1) with a thickness of about 5 nm [4,5]. Previous studies revealed that isolated S-layer subunits from *B. coagulans* E38-66/v1 recrystallize into large-scale closed arrays on various lipid films generated either by the Langmuir-technique [4,6,7] or on planar phospholipid bilayers [8–10].

S-layer-supported lipid membranes (Fig. 2; Ref. 11) mimic the cell envelope structure of gram-negative archaea possessing an S-layer as exclusive cell wall component external to the cytoplasm membrane [12]. From a general point of view, supported lipid membranes gain increasing importance in the development of biosensors [13–15] and in the characterization of functional transmembrane proteins. In previous studies, it was demonstrated that S-layer-supported lipid membranes are suitable to incorporate a large amount of sensing molecules without rupture [6,8], but also to perform single channel recordings [16–18].

In this context, it is interesting to note that mechanosensitive ion channels, like the family of epithelial Na^+-channels (ENaC), can be activated by a hydrostatic pressure difference [19]. For example, the α-bovine-ENaC showed a maximal single channel open probability at a hydrostatic pressure gradient of 9.5 N/m^2 [20]. With unsupported planar lipid membranes, however, the applied pressure gradient caused the formation of a new curved surface as it can be concluded from capacitance measurements. That is why there are two nonexclusive possibilities that can account for the activation of the channel: a curvature-induced mechanical activation or a water flow-induced activation [19]. Thus, to distinguish between the two activation mechanisms, there is a strong need for a composite lipid membrane that shows enhanced stability against bulging when a hydrostatic pressure is applied. The present work investigated the intrinsic features, in particular the change in capacitance, of unsupported and S-layer-supported bilayer lipid membranes in dependence of an applied hydrostatic pressure gradient. The results strongly suggest that S-layer-

* Corresponding author. Tel.: +43-1-47654-2200; fax: +43-1-4789112.
E-mail address: bschuste@edv1.boku.ac.at (B. Schuster).

0005-2736/02/$ - see front matter
PII: S0005-2736(02)00370-X

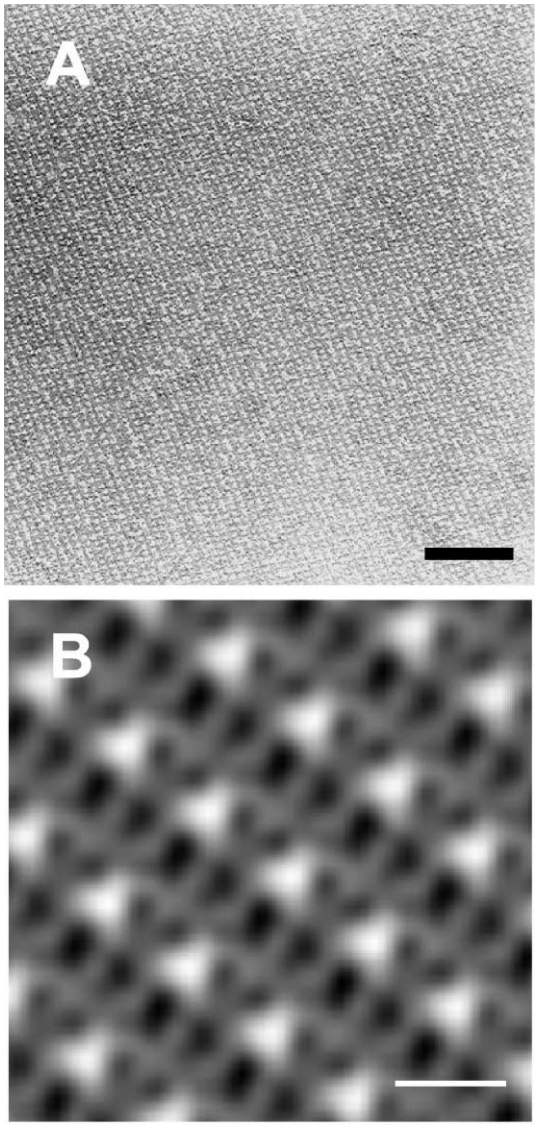

Fig. 1. (A) Electron micrograph of negatively stained preparation of the S-layer of *B. coagulans* E38-66/v1, recrystallized on a monolayer made of 1,2-diphytanoyl-*sn*-glycero-3-phosphatidylcholine (DPhPC)/hexadecylamine (HDA) (molar ratio 10:4). The bar corresponds to 100 nm. (B) Computer image reconstitution of the transmission electron microscopic images of the oblique S-layer lattice of *B. coagulans* E38-66/v1. The bar corresponds to 10 nm.

supported lipid membranes may be used as incorporation matrix with a significantly enhanced robustness against applied hydrostatic pressure gradients if the composite structure was pressurized from the protein-faced side.

2. Materials and methods

2.1. Generation of the lipid membrane

Black lipid membranes were made from a 1% (wt/wt) solution of a mixture (molar ratio 10:4) of DPhPC (Avanti Polar Lipids, Alabaster, AL, USA) and HDA in *n*-decane (both from Fluka, Buchs, Switzerland) as described elsewhere [21,22]. A custom-made polytetrafluoroethylene (Teflon) cuvette was separated into two cells (*cis* and *trans*) by a septum with an orifice 0.9 mm in diameter. The orifice was pre-painted with the same lipid mixture but dissolved in chloroform and dried with N_2 for at least 20 min. Both cells were filled with 12 ml buffer (2 mM $CaCl_2$, 10 mM KCl, adjusted with citric acid to pH 4.0) and equilibrated to guarantee equal buffer levels. The *cis*-cell was grounded, the *trans*-cell was connected by another Ag/AgCl-electrode to a voltage clamp set-up (EPC 9, HEKA Elektronik, Lambrecht/Pfalz, Germany). A drop of lipid mixture was put on a Teflon loop and was stroke up the orifice. Thinning of the lipid membranes was followed by capacitance measure-

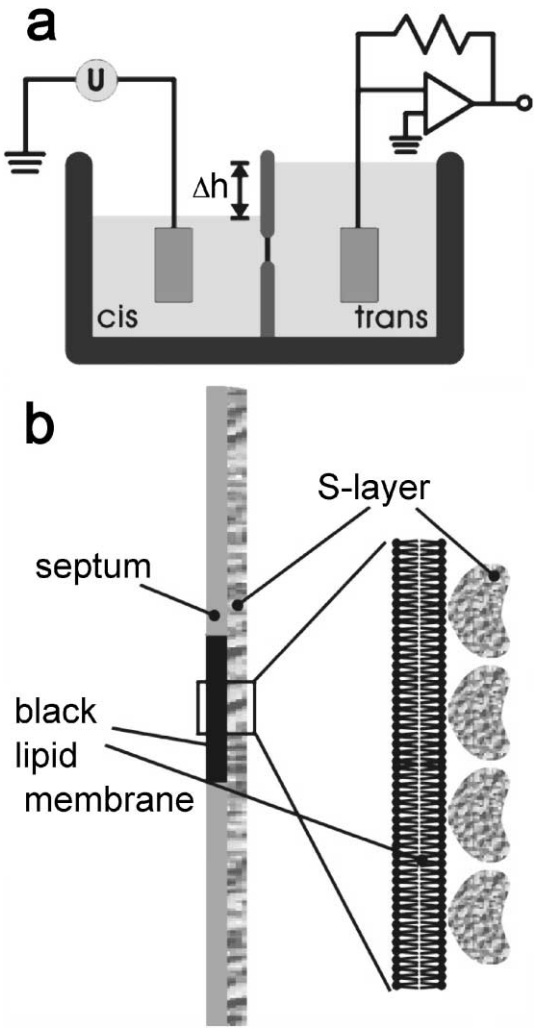

Fig. 2. Schematic view on the experimental set-up and of an S-layer-supported bilayer lipid membrane (not drawn to scale). In (a), the experimental set-up is shown. Each cell is contacted by an Ag/AgCl electrode. The hydrostatic pressure gradient is applied either by adding (not shown) or by removing electrolyte from the *cis*-cell. In (b), the architecture of the S-layer-supported lipid membrane is shown. On the bilayer lipid membrane, an S-layer lattice has been recrystallized from the *trans*-side.

ments and the experiments were started after reaching a constant value. The membrane conductance was usually $<10^{-8}$ S/cm^2. All experiments were performed at room temperature (22 ± 1 °C).

2.2. Recrystallization of the S-layer protein

Growth of *B. coagulans* E38-66/v1 in continuous culture, cell wall preparation and extraction of S-layer protein were performed as previously described [23]. The clear solution containing the disassembled S-layer subunits or oligomeric precursors (1.8 mg protein/ml) was used for all recrystallization experiments.

After membrane formation, the S-layer solution was carefully injected into the *trans*-cell of the cuvette to a final protein concentration of 0.2 mg/ml. The same volume of buffer was added to the *cis*-cell. The recrystallization process of S-layer subunits was completed within three hours [10]. In control experiments, S-layer protein was recrystallized on a monolayer of the same lipid composition. It is known that the lipid monolayer is a valid model also for lipid bilayer membranes as S-layer proteins recrystallize on both lipid films in the same time scale and quality [8]. After 3 hours, the composite structure was transferred on carbon-coated electron microscope grids. The negatively stained preparations were inspected by transmission electron microscopy (Philips CM12, Eindhoven, The Netherlands).

2.3. Set-up

The current response from given voltage functions was measured to provide the capacitance and conductance of unsupported and S-layer-supported bilayers. Data handling was performed on a Power Macintosh 7600/120 personal computer by the Pulse + PulseFit 8.11 software (HEKA Elektronik). Statistical analysis was performed using the Microcal ORIGIN program. The settings of the two built-in Bessel filters of the EPC 9 amplifier for the current-monitor signal were 10 and 1.5 kHz, respectively. A triangular voltage function (+40 to −40 mV, 20 ms) was used to determine the capacitance of the lipid membrane.

2.4. Application of the pressure gradient

Hydrostatic pressure was applied to lipid bilayers by asymmetrical addition or removal of buffer from the *cis*-cell by a syringe pump (SP120p, WPI, Sarasota, FL, USA) at a flow rate of 2 ml/h. The basal area of both cells was 7.1 cm^2, and thus, a volume change in one of the cells of 0.8 ml resulted in a difference in height of the buffer level of 1.13 mm. This difference in height, Δh (Fig. 2), corresponded to a hydrostatic pressure difference, ΔP, of 11.02 N/m^2 as determined from

$$\Delta P = \rho g \Delta h \quad (1)$$

with ρ, the specific weight of water at 22 °C (997 kg/m^3), and g, the acceleration due to gravity. Upon deformation, the membrane changes its area (ΔA) and possibly also its thickness, which can be monitored by a change in the capacitance (ΔC). As a change in thickness of the membrane is very unlikely because of the high value of Young's modulus [24–26], ΔA can be estimated from the measured ΔC by

$$\Delta A = \Delta C d / \varepsilon \varepsilon_0 \quad (2)$$

with d, the bilayer thickness, which is 4.5 nm [27], $\varepsilon = 2.1$, the dielectric constant of the membrane, and ε_0, the dielectric constant of free space. For curvature induced by the hydrostatic pressure difference ΔP across the planar lipid bilayer, the induced tension, T, is given by

$$T = \Delta P R / 2 \quad (3)$$

where R is the radius of the curvature of the bulged membrane, which can be calculated from ΔA [25,28–31].

3. Results

3.1. S-layer recrystallized on lipid films

In the present study, the S-layer protein of *B. coagulans* E38-66/v1 was recrystallized on planar phospholipid mono- and bilayers. Electron microscopical studies on lipid monolayers coated with S-layer proteins have shown large-scale closed monolayers of crystalline arrays (Fig. 1). The regularly structured S-layer had a crazy-paving appearance. All

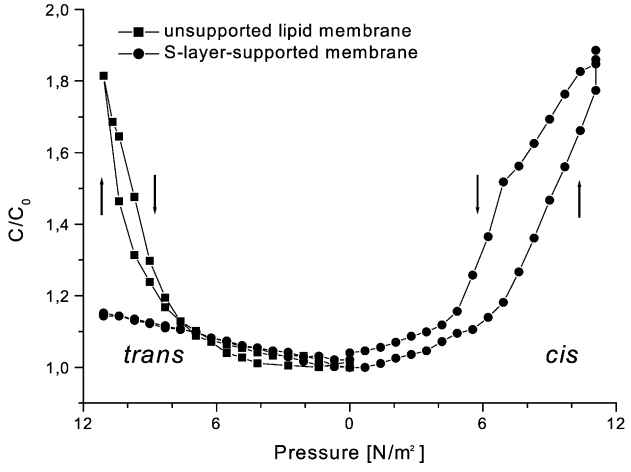

Fig. 3. Characteristic increase in capacitance upon application of an external hydrostatic pressure to the *trans*-side of unsupported (■) and to the *cis*- and *trans*-side of S-layer-supported lipid bilayer membranes (●). The up-arrow ↑ indicates that the hydrostatic pressure increased from 0 to 11.0 N/m^2, whereas the down-arrow ↓ indicates the decreasing pressure from the maximal to the initial value.

randomly oriented crystallites reached an average size of several micrometers. As previously mentioned, the lipid monolayer is a valid model system for lipid bilayers [8,10] and, thus, it can be concluded that the S-layer proteins recrystallized in the same quality on the bilayer lipid membranes.

3.2. Pressure application on unsupported lipid membranes

The capacitance of unsupported bilayer lipid membranes before the application of a hydrostatic pressure, C_0, was determined to be 1.8 ± 0.2 nF (number of experiment, $n = 21$). Subsequently a hydrostatic pressure from the *cis*- or *trans*-side was applied. No matter from which side the hydrostatic pressure acted, only minor effect on the measured capacitance was observed up to a pressure of ~ 6 N/m^2. Increasing the hydrostatic pressure from 6 to 11.0 N/m^2 resulted in a pronounced increase of the capacitance of the lipid membrane, C. Again, no difference was observed depending on which side the pressure was applied. For a better visualization, this behavior is shown in Fig. 3 for a hydrostatic pressure acting from the *trans*-side on the lipid membrane. The additional lipid needed for the increase of the membrane area is presumably supplied by the lipid of the annulus [32]. The highest ratio of the measured capacitance at a pressure of 11.0 N/m^2 divided by C_0, $C/C_{0,\max}$ was found to be 2.07 ± 0.3 ($n = 16$). As summarized in Table 1, the radius of curvature of the bulged membrane, R, was estimated to 0.46 mm and, thus, the lipid membrane has to be shaped semicircular. The induced tension caused by a ΔP of 11.0 N/m^2 was calculated to 2.5 mN/m (Table 1). Balancing the hydrostatic pressure resulted in a slightly higher value ($\sim 2\%$) than the initial capacitance. Further increase in pressure induced a huge increase in capacitance of up to five to eight times of the initial value and subsequently the membranes ruptured.

Table 1
Summary of the physical parameters of lipid bilayers with and without an attached S-layer lattice

	Bilayer, *cis*/*trans*	Bilayer + S-layer, *cis*	Bilayer + S-layer, *trans*
$r \times 10^4$ [m][a]	4.5	4.5	4.5
$d \times 10^9$ [m][b]	4.5	4.5	4.5
$\Delta P_{\max}$ [N/m^2]	11.02	11.02	11.02
$C/C_{0,\max}$	2.07 ± 0.30	1.87 ± 0.04	1.17 ± 0.05
$\Delta A_{\max} \times 10^7$ [m^2]	4.6 ± 0.6	3.4 ± 0.1	0.7 ± 0.03
$R_{\max} \times 10^4$ [m]	4.6 ± 0.6	4.7 ± 0.1	7.7 ± 0.3
$T_{\max}$ [mN/m]	2.5 ± 0.3	2.6 ± 0.1	4.3 ± 0.2

The radius of the aperture is r, d is the bilayer thickness, $\Delta P_{\max}$ is the maximal hydrostatic pressure difference across the planar lipid bilayer, $C/C_{0,\max}$ is the maximal ratio of the measured capacitance at $\Delta P_{\max}$ divided by the capacitance before the application of a hydrostatic pressure gradient, $\Delta A_{\max}$ and $R_{\max}$ are the maximal increase in area and in the radius of curvature of the bulged membrane, induced by $\Delta P_{\max}$, respectively, and $T_{\max}$ is the maximal induced tension.

[a] One aperture was used in all experiments.

[b] Value was taken from Ref. [27].

3.3. Pressure application on S-layer-supported lipid membranes

After recrystallization of the S-layer protein of *B. coagulans* E38-66/v1 on the *trans*-side of the lipid membrane, the measured C_0 of the composite membrane was 1.6 ± 0.1 nF ($n = 17$), resembling the values determined for unsupported lipid membranes. The application of a hydrostatic pressure from the *cis*-, lipid-faced side induced an increase of the capacitance (Fig. 3). As observed with unsupported lipid membranes, C/C_0 increased slowly at low pressures. At a higher hydrostatic pressure, C/C_0 increased faster and reached finally a $C/C_{0,\max}$ of 1.87 ± 0.04 ($n = 6$) at a pressure of 11.0 N/m^2. R was found to be similar to that of unsupported lipid membranes and the induced tension was with 2.6 mN/m only slightly higher than that of the latter one (Table 1). The capacitance of the membrane, C, decreased upon reduction of the pressure, although at zero pressure, it was about 4% higher than the initial value. The most pronounced effect of the attached S-layer was observed at the application of a hydrostatic pressure from the *trans*-side, the S-layer face of the composite membrane. C/C_0 increased very slowly and reached the maximal value of 1.17 ± 0.05 ($n = 6$) at a pressure of 11.0 N/m^2 (Table 1). In this case, R was significantly higher compared to the previously described experimental series (Table 1). Thus, the lipid membrane was bulged to a much lower extent and the induced tension was calculated to 4.3 mN/m. By balancing the pressure difference, the capacitance of the composite structure returned to a value slightly higher ($\leq 2\%$) than the initial one (Fig. 3).

4. Discussion

In the present study, a hydrostatic pressure gradient was applied to unsupported and S-layer-supported lipid membranes. The effect of a closely attached S-layer lattice on the deformation was measured by the change of the capacitance of the lipid membrane. The symmetric unsupported lipid membrane, pressurized from the *cis*- or from the *trans*-side, and the asymmetrically formed S-layer-supported lipid membrane, pressurized from the lipid-faced, *cis*-side revealed similar values for $C/C_{0,\max}$. As R was found to be very close to the radius of the aperture, the bulged membrane must have an almost semicircular shape (Table 1). A higher hydrostatic pressure would most probably result in a cigar-shaped structure, which is obviously not stable as the capacitance increased not reproducibly and the membrane ruptured as determined with unsupported lipid membranes. The pressure-induced tension was, for both membranes at the previously described conditions, in the range of ~ 2.6 mN/m and thus, in the range reported for other painted

bilayer lipid membranes [25,33]. However, a significantly less maximal increase in area (Table 1) and a more pronounced hysteresis at the pressure versus capacitance plot was observed for the S-layer-supported lipid membrane pressurized from the *cis*-side compared to unsupported membranes (Fig. 3). Applying a pressure from the lipid face resulted in bulging of the S-layer together with the lipid membrane away from the Teflon septum. A previous study demonstrated that the S-layer protein recrystallized not only on the membrane spanning the aperture, but also on the Teflon septum in the vicinity of the hole, which is lipid-coated from the pre-painting [8]. The observed slight hysteresis might be explained by a rearrangement of the closed S-layer lattice into patches at few places, including the edge of the aperture. By balancing the pressure, the composite membrane returned into the planar shape, but the S-layer patches might require some time to reorient into the original, closed lattice structure. Another possibility might be that the S-layer lattice did not disintegrate into patches and the additional composite structure was provided from the vicinity of the aperture. Again, a certain time might be required for the relaxation of the S-layer-supported lipid membrane into its planar shape.

A totally different behavior was observed for the asymmetric S-layer-supported lipid membrane pressurized from the protein-faced, *trans*-side. $C/C_{0,\max}$ was significantly lower than that of unsupported and S-layer-supported lipid membranes pressurized from the opposite, lipid-faced side. X-ray and neutron reflectometry measurements on S-layer-supported Langmuir films demonstrated that peptide material interpenetrated the phospholipid head group region in its entire depth but did not affect the hydrophobic lipid acyl chains [34,35]. The head group region of the adjacent lipid monolayer is modulated by the S-layer in terms of a reduced hydration, altered orientation and fluidity, and increased surface viscosity and bending stiffness [7,9,35]. In S-layer-supported lipid membranes, two components (opposite lipid leaflet and lipid leaflet with the closely attached S-layer lattice) with different intrinsic physicochemical features are linked primarily by hydrophobic forces. In addition, the S-layer from *B. coagulans* E38-66/v1 revealed a pronounced asymmetry of the topography and physicochemical properties of the two faces oriented to the bacterial cell wall (‘‘inner face’’) or pointing away to the environment (‘‘outer face’’) [4,5]. The inner, more corrugated face of the S-layer lattice is electrostatically and via specific interactions linked to the adjacent lipid monolayer [7,35]. Due to the topographical feature of the inner S-layer surface, repetitive contact sites in approximately 2 nm dimensions have been estimated. Consequently, detaching of the lipid membrane from the S-layer cannot be expected. Although the three-dimensional structure of the S-layer lattice at atomic resolution is not known, the S-layer lattice itself may posses different robustness when a hydrostatic pressure is applied from the inner or outer surface, particular in combination with the attached lipid membrane. The maximal induced tension calculated for an S-layer-supported lipid membrane reflects the difference in bending stiffness depending on the side of application of the hydrostatic pressure gradient. The induced tension of the composite membrane, pressurized from the *trans*-side, was more than 65% higher compared to a pressure acting from the opposite side (Table 1). Thus, this observation strengthen the assumption made above. In addition, no hysteresis in the pressure versus capacitance relationship, which refers to the absence of significant rearrangements of components of the S-layer-supported lipid membrane, was observed.

Summarizing these results, the S-layer-supported lipid membrane pressurized from the protein-faced side was able to maintain its shape to a much higher extent, particularly in a pressure range of 8 to 11 N/m^2. Consequently, these composite membranes might be used for the reconstitution of mechanosensitive ion channels, like ENaC, whenever a reduction of the curvature-induced activation is desired [36]. Based on the present data, it was not possible to figure out explanations on the molecular level. Further studies with less complex structures like Langmuir films will be necessary to understand the observations in more detail. With this first insight into the intrinsic features of S-layer/lipid membranes upon application of hydrostatic pressure gradients, further work as well with functionalized membranes will be the focus of future research.

Acknowledgements

We are grateful to J. Friedmann for technical assistance and D. Pum for the computer image reconstitution. This work was supported by the Ludwig Boltzmann Society, by grants from the Austrian Science Foundation, Project 14419-MOB, and by the Volkswagen Foundation, Germany, Project I/77 710.

References

[1] M. Sára, U.B. Sleytr, J. Bacteriol. 182 (2000) 859–868.
[2] U.B. Sleytr, P. Messner, D. Pum, M. Sára, Angew. Chem., Int. Ed. 38 (1999) 1034–1054.
[3] U.B. Sleytr, M. Sára, D. Pum, B. Schuster, in: M. Rosoff (Ed.), Nano-Surface Chemistry, Marcel Dekker, New York, 2001, pp. 333–389.
[4] D. Pum, M. Weinhandl, C. Hödl, U.B. Sleytr, J. Bacteriol. 175 (1993) 2762–2766.
[5] M. Sára, D. Pum, U.B. Sleytr, J. Bacteriol. 174 (1992) 3487–3493.
[6] B. Schuster, D. Pum, U.B. Sleytr, Biochim. Biophys. Acta, Biomembr. 1369 (1998) 51–60.
[7] B. Wetzer, A. Pfandler, E. Györvary, D. Pum, M. Lösche, U.B. Sleytr, Langmuir 14 (1998) 6899–6906.
[8] B. Schuster, D. Pum, O. Braha, H. Bayley, U.B. Sleytr, Biochim. Biophys. Acta, Biomembr. 1370 (1998) 280–288.
[9] R. Hirn, B. Schuster, U.B. Sleytr, T.M. Bayerl, Biophys. J. 77 (1999) 2066–2074.
[10] B. Schuster, U.B. Sleytr, A. Diederich, G. Bähr, M. Winterhalter, Eur. Biophys. J. 28 (1999) 583–590.
[11] B. Schuster, U.B. Sleytr, Rev. Mol. Biotechnol. 74 (2000) 233–254.
[12] U.B. Sleytr, T.J. Beveridge, Trends Microbiol. 7 (1999) 253–260.

[13] H.T. Tien, A.L. Ottova, J. Membr. Sci. 189 (2001) 83–117.
[14] E. Sackmann, M. Tanaka, Trends Biotechnol. 18 (2000) 58–64.
[15] D.P. Nikolelis, T. Hianik, U.J. Krull, Electroanalysis 11 (1999) 7–15.
[16] B. Schuster, U.B. Sleytr, Bioelectrochemistry 55 (2002) 5–7.
[17] B. Schuster, D. Pum, M. Sára, O. Braha, H. Bayley, U.B. Sleytr, Langmuir 17 (2001) 499–503.
[18] H. Bayley, P.S. Cremer, Nature 413 (2001) 226–230.
[19] I.I. Ismailov, V.G. Shlyonsky, D.J. Benos, Proc. Natl. Acad. Sci. U. S. A. 94 (1997) 7651–7654.
[20] M.S. Awayda, I.I. Ismailov, B.K. Berdiev, D.J. Benos, APStracts 2 (1995) 49.
[21] P. Mueller, O.D. Rudin, H.T. Tien, W.C. Wescott, J. Phys. Chem. 67 (1963) 534–541.
[22] R. Fettiplace, L.G.M. Gordon, S.B. Hladky, J. Requena, H.P. Zingsheim, D.A. Haydon, in: E.D. Korn (Ed.), Methods of Membrane Biology, vol. 4, Plenum, New York, 1975, pp. 1–75.
[23] U.B. Sleytr, M. Sára, Z. Küpcü, P. Messner, Arch. Microbiol. 146 (1986) 19–24.
[24] G. Cevc, D. Marsh, in: E.E. Bittar (Ed.), Cell Biology: A Series of Monographs, vol. 5, Wiley, New York, 1987, pp. 347–368.
[25] R. Benz, O. Frohlich, P. Lauger, M. Montal, Biochim. Biophys. Acta 394 (1975) 323–334.
[26] D. Needham, R.M. Hochmuth, Biophys. J. 55 (1989) 1001–1009.
[27] J. Stern, H.J. Freisleben, S. Janku, K. Ring, Biochim. Biophys. Acta 1128 (1992) 227–236.
[28] D. Marsh, Handbook of Lipid Bilayers, CRC Press, Boca Raton, 1990, pp. 195–197.
[29] D. Marsh, Biochim. Biophys. Acta 1286 (1996) 183–223.
[30] D. Needham, R.S. Nunn, Biophys. J. 58 (1990) 997–1009.
[31] E. Sackmann, in: R. Lipowsky, E. Sackmann (Eds.), Structure and Dynamics of Membranes, Elsevier, Amsterdam, 1995, pp. 213–304.
[32] S.H. White, in: C. Miller (Ed.), Ion Channel Reconstitution, Plenum, New York, 1986, pp. 3–36.
[33] S.H. White, Biophys. J. 15 (1975) 95–117.
[34] M. Weygand, B. Wetzer, D. Pum, U.B. Sleytr, N. Cuvillier, K. Kjaer, P.B. Howes, M. Lösche, Biophys. J. 76 (1999) 458–468.
[35] M. Weygand, M. Schalke, P.B. Howes, K. Kjaer, F. Friedmann, B. Wetzer, D. Pum, U.B. Sleytr, M. Lösche, J. Mater. Chem. 10 (2000) 141–148.
[36] S.W. Hui, in: R.M. Epand (Ed.), Lipid Polymorphism and Membrane Properties, Current Topics in Membranes, vol. 44, Academic Press, San Diego, 1997, pp. 541–563.